Journal of Alloys and Compounds 509 (2011) 3711–3715

Contents lists available at ScienceDirect

Journal of Alloys and Compounds

journal homepage: www.elsevier.com/locate/jallcom

A novel method to synthesize anatase TiO_2 nanowires as an anode material for lithium-ion batteries

Feixiang Wu, Xinhai Li*, Zhixing Wang, Huajun Guo, Ling Wu, Xunhui Xiong, Xiaojuan Wang

School of Metallurgical Science and Engineering, Central South University, Changsha 410083, PR China

ARTICLE INFO

Article history:
Received 9 November 2010
Received in revised form
20 December 2010
Accepted 25 December 2010
Available online 31 December 2010

Keywords:
Lithium ion batteries
Anatase
Titanium dioxide
Anode material
Nanowires

ABSTRACT

We demonstrate a simple and novel approach for the synthesis of a kind of anatase TiO_2 nanowires. The method is based on a hydrothermal method under normal atmosphere without using the complex Teflon-lined autoclave, high concentrations NaOH solution and long react time. The as-prepared materials are characterized by X-ray diffraction (XRD), scanning electron microscopy (SEM) and electrochemical measurements. The obtained anatase TiO_2 nanowires show excellent performance. There is a potential plateau at 1.77 and 1.88 V in the process of Li insertion and extraction, and the initial Li insertion/extraction capacities are 283 and 236 mAh g^{-1} at the density of 20 mA g^{-1}, respectively. In the 20th cycle, the reversible capacities still remain about 216 and 159 mAh g^{-1} at the current densities of 20 and 200 mA g^{-1}, respectively, and the coulombic efficiency is more than 98%, exhibiting excellent electrochemical performance.

1. Introduction

Rechargeable lithium-ion cells are key components of the portable, entertainment, computing, and telecommunication equipment because of their high-energy storage density, high voltage, long cycle life, high-power sources, and ambient temperature operation [1,2]. In this area, cathode materials have been widely studied, such as $LiMn_2O_4$, $LiCoO_2$, $LiNi_{1/3}Mn_{1/3}Co_{1/3}O_2$, $LiFePO_4$, etc. [3–6]. However, the anode materials also play an important role in the lithium-ion batteries. The carbon negative electrode used in rechargeable lithium-ion cells suffers from a number of problems; most notably the potential for lithium intercalation is close to that of the Li^+/Li redox couple, leading to the possibility of lithium plating during charge and hence significant safety concerns, also charge must be consumed in order to form the SEI layer (essential to the operation of the carbon electrode) on the first charge cycle. Titanium oxide (TiO_2) is probably the most widely studied semiconducting metal oxides due to its great application potential in many fields, such as photocatalysis, sensors, solar cells, and lithium–ion batteries.

Nanoscale materials often exhibit physical and chemical properties that differ greatly from their bulk counterpart [7]. Therefore, nanostructured TiO_2 has been widely investigated as a key material in fundamental research and technological applications in the fields of optical devices, photovoltaic cells, photocatalysts, gas sensing, and electrochemical storage [8–11]. Particularly, much attention has been paid to nanostructured TiO_2 for Li-insertion, because it is not only a low-voltage insertion host for Li^+, but also a fast Li-insertion/extraction host. These characteristics render it a potential anode material for lithium-ion batteries [12–14].

Recently, nanotubular TiO_2, TiO_2 nanorods, and TiO_2 (B) nanowires have been studied by many researchers. They always mixed the TiO_2 nanoparticles and high concentrations NaOH solution (or HF solution), and added the mixture into Teflon-lined autoclave to be autoclaved at 110 ~ 200 °C for 24 ~ 72 h [15–21]. According to S.Z. Makarov's report, $Ti(OH)_4$ can react with H_2O_2 to form the compound $TiO_3{\cdot}2H_2O$. The compound of the composition $TiO_3{\cdot}2H_2O$ should be written in the form $Ti(OOH)(OH)_3$, since it can be regarded as a derivative of $Ti(OH)_4$ with one hydroxyl group replaced by a perhydroxyl (OOH) ground [22].This method using coordination agent of H_2O_2 is widely used in catalyst and photocatalysis fields to obtain nanosize TiO_2 thin film [23–25]. In Mitsunori Yada's report, titania and titanate nanofiber were synthesized by mixing peroxotitanic acid solution with NaOH aqueous solution [26]. In our previous study, we use the hydrogen peroxide as a coordination agent which can provide a kind of ligand (O_2^{2-} ion) to dissolve Ti from the hydrolyzed titania precipitate. Several O_2^{2-} ions can react with the Ti of high-titanium precipitate to form a large anion in which Ti is taken as the central ion and can exist stably in the alkaline solution. The coordination agent of H_2O_2 is firstly used in leaching of hydrolyzed titania residue decomposed from mechanically activated Panzhihua ilmenite leached by hydrochlo-

* Corresponding author. Tel.: +86 731 88836633; fax: +86 731 88836633.
E-mail address: feixiang0929@163.com (X. Li).

0925-8388/$ – see front matter © 2010 Elsevier B.V. All rights reserved.
doi:10.1016/j.jallcom.2010.12.182

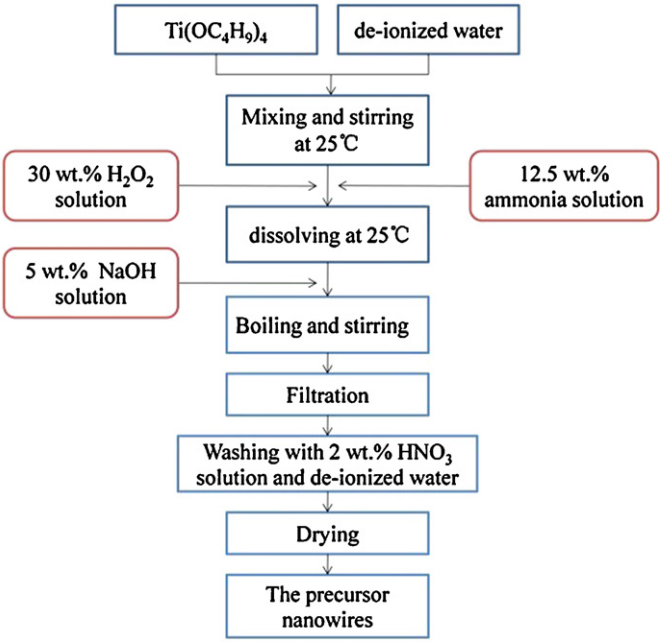

Fig. 1. The experimental procedure.

ric acid [27]. This method using coordination agent of H_2O_2 has not been used in prepartion of TiO_2 nanowires at present. In this paper, we propose a novel, simple and improved route for obtaining the TiO_2 nanowires by means of simple boiling of titanium peroxide solution instead of hydrothermal treatment of TiO_2 in alkaline solutions. Anatase TiO_2 nanowires with excellent electrochemical performance can be successfully synthesized without using the complex Teflon-lined autoclave, high concentrations NaOH solution and long react time.

2. Experimental

2.1. Synthesis and characterization

Anatase TiO_2 nanowires were synthesized by adding 15 g of $Ti(OC_4H_9)_4$ to a 100 ml de-ionized water in the 250 ml beaker and white slurry was observed. After stirring for 5 min, 20 g of 30 wt.% H_2O_2 solution was added into the beaker and ammonia solution (12.5 wt.%) was added into the beaker to maintain pH value near 10.5. After about 40 min, the white slurry was dissolved to form a yellow-green solution, and then transferred to a 1000 ml Beaker. After that, 400 g of 5 wt.% NaOH solution was added into the beaker, and then boiled to boiling point under vigorous stirring in an oil bath. One hour later, the white slurry was formed and filtrated. The obtained precipitate was washed 2 times with 2 wt.% HNO_3 solution, then washed with de-ionized water several times. Finally, the white product was dried at 120 °C for more than 8 h and the precursor was obtained. Further, the dried precursor was calcined at 400 °C for 3 h in air to obtain anatase TiO_2 nanowires. The experimental procedure was shown in Fig. 1.The precursor nanowires and TiO_2 nanowires were analyzed using inductively coupled plasma emission spectroscopy (ICP, IRIS intrepid XSP, Thermo Electron Corporation). The SEM images of the particles were observed with scanning electron microscopy (SEM, Sirion 200). The powder X-ray diffraction (XRD, Rint-2000, Rigaku) using CuKα radiation was employed to identify the crystalline phase of the precursor and TiO_2 nanowires. The elements on the surface of samples were identified by energy-dispersive X-ray spectroscopy (EDS).

2.2. Electrochemical measurement

The electrochemical performance was performed using a two-electrode cointype cell (CR2025) of Li,$LiPF_6$ (EC: EMC: DMC = 1: 1: 1 in volume),TiO_2. The working cathode was composed of 80 wt.% TiO_2 powders, 10 wt.% acetylene black as conducting agent, and 10 wt.% poly (vinylidene fluoride) as binder. After being blended in N-methyl pyrrolidinone, the mixed slurry was spread uniformly on a thin copper foil and dried in vacuum for 12 h at 120 °C. A metal lithium foil was used as the anode. Electrodes were punched in the form of 14 mm diameter disks, and the typical positive electrode loading was about 1.95 mg/cm^2. A polypropylene microporous film was used as the separator. The assembly of the cells was carried out in a dry argon-filled glove box. The cells were charged and discharged over a voltage range of 1.0–3.0 V versus Li/Li^+ electrode at room temperature.

3. Results and discussion

3.1. Morphology and structure of the materials

Fig. 2 shows SEM images of the precursor (a, b) and as-prepared TiO_2 (c, d). From the Fig. 2(b and d), porous spherical particles or microspheres with a diameter of 500–700 nm and rough surface are observed obviously chestnut-like morphology which is firstly reported in our paper. Two enlarged images of the particles of the precursor and as-prepared TiO_2 indicate that the spherical particles or microspheres are composed of aggregations of nanowires (Fig. 2(a and c)). The precursor is calcined at 400 °C for 3 h to synthesize TiO_2. As shown in Fig. 2, the morphology images of the precursor and as-prepared TiO_2 are the similar nanowires structure. These nanowires are of diameter 20 nm and can extend up to 250 nm in length. Compared with other nanostructured TiO_2, the unique morphology would make the active material contact with electrolyte more sufficiently, which improve the electrochemical property.

Fig. 3 shows the XRD patterns of the precursor and as-prepared TiO_2. According to Ma's report, the peaks of the precursor nanowires marked in curve (Fig. 3(a)) can be readily indexed to a lepidocrocite-type titanate phase (e.g., orthorhombic $H_xTi_{2-x/4\gamma x/4}O_4{\cdot}H_2O$, here $x \approx 0.7$, γ: vacancy, $a = 0.3783$ nm, $b = 1.8735$ nm and $c = 0.2978$ nm) [28]. The broad peaks at $2\theta = 8.85°$, 24.1°, 27.8°, 48.3° and 61.7° correspond well with (0 2 0), (1 1 0), (1 3 0), (2 0 0) and (0 0 2) reflections of the lepidocrocite titanates. Fig. 3(b) displays the diffraction peaks of as-prepared TiO_2 from the precursor nanowires. The as-prepared TiO_2 with high crystallinity is well ascribed to the (1 0 1), (1 1 0), (2 0 0), (2 1 1), (2 0 4), (1 1 6) and (2 1 5) diffraction peaks of anatase TiO_2 [29]. It indicates that after calcined at 400 °C for 3 h, the structure of the precursor nanowires has changed into anatase TiO_2 nanowires. The anatase nanostructured TiO_2 which facilitates the insertion/extraction of Li^+ during discharge/charge would exhibit excellent electrochemical performance. ICP analysis reveals that Na and other impurity elements are not detected in the precursor and as-prepared TiO_2. We also detect elements on the surface of samples by EDS. As shown in Fig. 3(c and d), Na and other impurity elements are absent in the precursor and as-prepared TiO_2, which are consistent with the ICP results.

3.2. Electrochemical performance

Fig. 4(a) shows the initial three potential-capacity profiles of anatase TiO_2 nanowires at the charge/discharge current density of 20 mA g^{-1}. There are distinct potential plateaus at 1.77 and 1.88 V for discharging and charging, respectively. A similar potential plateaus have also been observed in other literatures [30,31]. In the first discharge process, the anatase TiO_2 nanowires electrode exhibites a remarkably high initial discharge capacity at a current density of 20 mA g^{-1}, up to 283 mAh g^{-1}, which is near the stoichiometry Li/Ti = 0.84. Compared with traditional materials, the larger capacity obtained may be ascribed to a shorter diffusion length for both the electron and Li^+, and a larger electrode/electrolyte contact area of TiO_2 nanowires which facilitate the lithium ions' insertion and extraction. The subsequent Li^+ extraction, proceeding up to 3.0 V, shows a capacity of 236 mAh g^{-1}, with a relatively low coulombic efficiency (ratio of exaction to insertion capacity) of 82% and a large irreversible capacity (47 mAh g^{-1}). However, in the subsequent two cycles, the discharge/charge curves are almost coincided with each other, indicating a low irreversible capacity and a higher coulombic efficiency. From Fig. 4(b and c), the discharge specific capacities

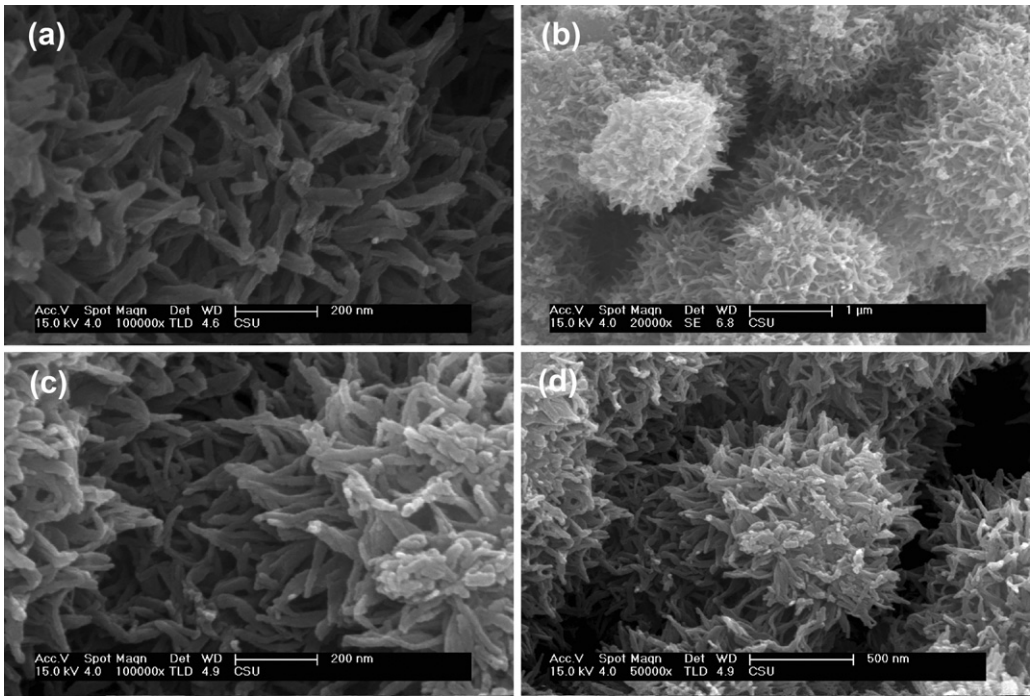

Fig. 2. SEM images of the precursor (a, b) and as-prepared TiO_2 (c, d); the enlarged images of the precursor (a) and as-prepared TiO_2 (c).

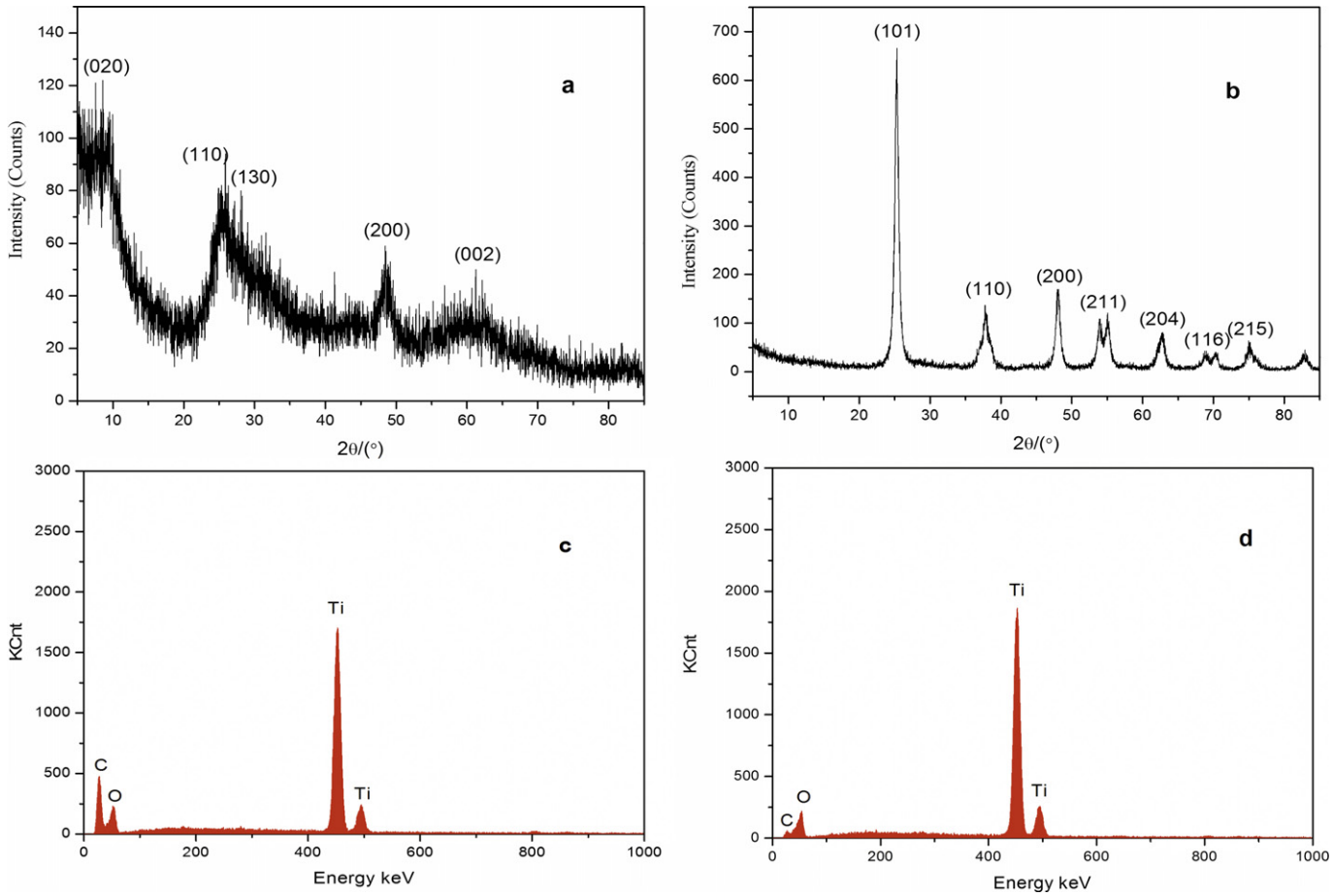

Fig. 3. XRD patterns of the precursor (a) and as-prepared TiO_2 (b); EDS patterns of the precursor (c) and as-prepared TiO_2 (d).

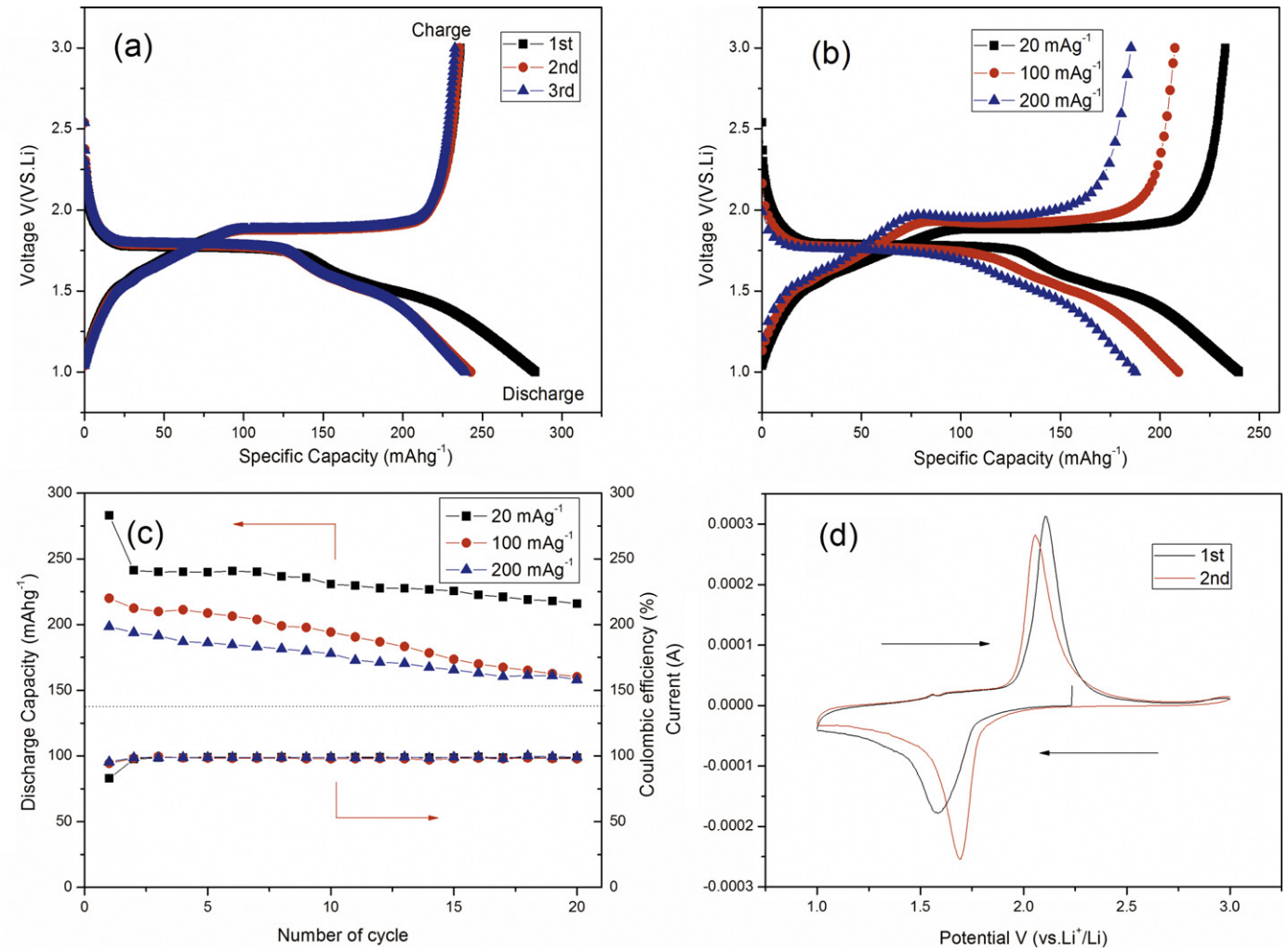

Fig. 4. (a) First three potential-capacity profiles of anatase TiO_2 nanowires at the charge/discharge current density of 20 mA g^{-1}; (b) Fifth cycle discharge–charge capacity of the anatase TiO_2 nanowires at the different current densities; (c) Variation of discharge capacity and coulombic efficiency with the number of cycles for the anatase TiO_2 nanowires at the different current densities; (d) Representative cyclic voltammogram plots of anatase TiO_2 nanowires electrodes at 0.1 mV s^{-1}.

of 238, 209 and 189 mAh g^{-1} are obtained at the current densities of 20, 100 and 200 mA g^{-1}. After a relatively large capacity drop in the first cycle, the capacity in the second cycle was still great (241 mAh g^{-1}). This anatase TiO_2 nanowires exhibits a favorable cycling capability during the subsequent charge/discharge, namely, almost 90.5% discharge capacity retention, from the 2nd to the 20th cycle. At the higher current densities, after 20 cycles, this anode marerial retains 75% of its initial discharge capacity (220 mAh g^{-1}) and retains 80% of its initial discharge capacity (198 mAh g^{-1}) at the current densities of 100 and 200 mA g^{-1}, respectively. According to the variation of coulombic efficiency (Fig. 4(c)), at all the current densities, the coulombic efficiencies reach more than 98% after the first cycle and gradually increase to 100%. It suggests the high reversibility and stability of Li-intercalation and de-intercalation for the anatase TiO_2 nanowires, which is also shown in Fig. 4(d). As shown, in the first cycle, there is a pair of cathodic/anodic peaks centered at 1.57 and 2.07 V, corresponding to the lithium insertion/extraction in anatase TiO_2 lattice, respectively. In the second cycle, there is a sharp single pair of cathodic/anodic peaks located at 1.7 and 2.14 V with well-defined shoulders. The cathodic and anodic peaks are in accordance with the plateaus of the discharging/charging curves. The measured value of the ratio for peak currents i_{pa}/i_{pc} is nearly 1, and the integral voltammetric area of the discharging/charging branches is almost equal, indicating a very perfect coulombic efficiency. These demonstrate that the anatase TiO_2 nanowires exhibit excellent electrochemical performance.

4. Conclusions

In summary, the anatase TiO_2 nanowires are synthesized by a simple and novel hydrothermal method without using the complex Teflon-lined autoclave, high concentrations NaOH solution and long react time. Owing to its' special nanostructure, the anatase TiO_2 nanowires have excellent electrochemical performance. There are long voltage plateaus in the discharging/charging curves. Cycling efficiency is excellent, as is the capacity retention on cycling after an irreversible capacity on the first cycle. The coulombic efficiency more than 98% and the good symmetry of the cyclic voltammogram reveal excellent reversibility. This anode material also presents good cycling performance. The high-performance anatase TiO_2 nanowires anode material coupled with the simple, low temperature, less react time, low cost, and environmentally benign nature of the preparation method may make this material attractive for large applications.

Acknowledgement

The project was sponsored by the National Basic Research Program of China (973 Program, 2007CB613607).

References

[1] J.M. Tarascon, M. Armand, Nature 414 (2001) 359–367.
[2] M.S. Whittingham, Chem. Rev. 104 (2004) 4271–4301.
[3] Y.K. Li, R.X. Zhang, J.S. Liu, C.W. Yang, J. Power Sources 189 (2009) 685–688.
[4] Z.H. Chen, J.R. Dahn, Electrochim. Acta 49 (2004) 1079–1090.
[5] W.B. Luo, X.H. Li, J.R. Dahn, J. Electrochem. Soc. 157 (7) (2010) A782–A790.
[6] L. Wu, X.H. Li, Z.X. Wang, L.J. Li, J.C. Zheng, H.J. Guo, Q.Y. Hu, J. Fang, J. Power Sources 189 (2009) 681–684.
[7] A.P. Alivisatos, Science 271 (1996) 933–937.
[8] B. O'Regan, M. Gr¨atzel, Nature 353 (1991) 737–740.
[9] G.K. Boschloo, A. Goossens, J. Schoonman, J. Electrochem. Soc. 144 (1997) 1311–1317.
[10] Y. Li, D.S. Hwang, N.H. Lee, S.J. Kim, Chem. Phys. Lett. 404 (2005) 25–29.
[11] S.U.M. Khan, M. Al-Shahry, W.B. Ingler, Science 297 (2002) 2243–2245.
[12] L. Kavan, M. Gr¨atzel, S.E. Gilbert, C. Klemenz, H.J. Scheel, J. Am. Chem. Soc. 118 (1996) 6716–6723.
[13] I. Exnar, L. Kavan, S.Y. Huang, M. Gr¨atzel, J. Power Sources 68 (1997) 720–722.
[14] Y.S. Hu, L. Kienle, Y.G. Guo, J. Maier, Adv. Mater. 18 (2006) 1421–1426.
[15] J.W. Xu, C.H. Jia, B. Cao, W.F. Zhang, Electrochim. Acta 52 (2007) 8044–8047.
[16] H. Zhang, X.P. Gao, G.R. Li, T.Y. Yan, H.Y. Zhu, Electrochim. Acta 53 (2008) 7061–7068.
[17] G. Armstrong, A.R. Armstrong, J. Canales, P.G. Bruce, Electrochem. Solid-State Lett. 9 (3) (2006) A139–A143.
[18] M.D. Wei, Z.M. Qi, M. Ichihara, I.H. Honma, S. Zhou, Chem. Phys. Lett. 424 (2006) 316–320.
[19] A.R. Armstrong, G. Armstrong, J. Canales, P.G. Bruce, J. Power Sources 146 (2005) 501–506.
[20] S.J. Bao, Q.L. Bao, C.M. Li, Z.L. Dong, Electrochem. Commun. 9 (2007) 1233–1238.
[21] J.S. Chen, X.W. Lou, Electrochem. Commun. 11 (2009) 2332–2335.
[22] S.Z. Makarov, L.V. Ladeinova, Russ. Chem. Bull. 10 (1961) 889–893.
[23] M.V. Shankar, T. Kako, D.F. Wang, J.H. Ye, J. Colloid Interface Sci. 31 (2009) 132–137.
[24] N. Sasirekha, B. Rajesh, Y.W. Chen, Thin Solid Films 518 (2009) 43–48.
[25] L. Ge, M.X. Xu, H.B. Fang, M. Sun, Appl. Surf. Sci. 253 (2006) 720–725.
[26] M. Yada, Y. Goto, M. Uoto, J. Eur. Ceram. Soc. 26 (2006) 673–678.
[27] F.X. Wu, X.H. Li, Z.X. Wang, Int. J. Miner. Process. 98 (2011) 106–112.
[28] R.Z. Ma, Y. Bando, T. Sasaki, Chem. Phys. Lett. 380 (2003) 577–582.
[29] B.L. He, B. Dong, H.L. Li, Electrochem. Commun. 9 (2007) 425–430.
[30] S.Y. Huang, L. Kavan, I. Exnar, M. Gratzel, J. Electrochem. Soc. 142 (1995) L142–144.
[31] A. Stashans, S. Lunell, R. Bergstrom, A. Hagfeldt, Lindquist S.E., Phys. Rev. B 53 (1996) 159–170.